Quantitative Analysis and Design of a Rudder Roll Damping Controller

Hearns, G.; Blanke, M.

Publication date:
1998

Document Version
Også kaldet Forlagets PDF

Link to publication from Aalborg University

Citation for published version (APA):
Hearns, G., & Blanke, M. (1998). *Quantitative Analysis and Design of a Rudder Roll Damping Controller*.

QUANTITATIVE ANALYSIS AND DESIGN OF A RUDDER ROLL DAMPING CONTROLLER

Gerald Hearns [*,1] **Mogens Blanke** [**]

[*] *Industrial Control Centre, Strathclyde University, Glasgow, UK*
[**] *Dept. of Control Engineering, Aalborg University, Denmark*

Abstract: A rudder roll damping controller is designed using Quantitative feedback theory to be robust for changes in the ships metacentric height. The analytical constraint due to the non-minimum phase behaviour of the rudder to roll is analysed using the Poisson Integral Formula and it is shown how the design tradeoffs in closed-loop roll reduction can be approximated using this formula before a controller is designed. The robust roll and course keeping controllers designed are then tested using a nonlinear simulation.

Keywords: Ship control, Robust performance, Non-minimum phase

1. INTRODUCTION

Reducing the roll on a cargo ship will prevent damage to the cargo and reduce the discomfort of the crew increasing their efficiency. Using the rudder for simultaneous course keeping and roll reduction is not a trivial problem since there is only one actuator thus requiring that the two objectives are separated in the frequency domain. This single input-multi output problem is also non-minimum phase or has a right half plane (RHP) zero in the channel from the rudder to the roll. RHP-zeros are typically caused by the effects of competing slow and fast dynamics. In this case the zero is produced by the roll moment exerted on the ship by the rudder competing with the sway force from the rudder to the roll moment. RHP-zeros are responsible for the initial inverse response to a step input and phase-lag in the frequency domain. We are interested in the RHP-zero because it imposes some fundamental constraints on the feedback system. To reduce the sensitivity of a system with a RHP-zero will mean that the benefits of feedback will be lost in another frequency region resulting in a sensitivity there with a peak greater than unity. This means there is an inherent design tradeoff as a consequence of the systems physical properties. The worst case would occur if the zero was in the same location as the frequency region which roll reduction is required.

The analytical constraint due the RHP-zero will be examined using the Poisson Integral Formula to predict the roll amplification if the roll is reduced in another frequency region. This formula enables the possible closed-loop roll sensitivities to be examined before a controller is designed. To design roll and course keeping controllers **Q**uantitatvie **F**eedback **T**heory will be used since it enables the design tradeoffs and robustness to be easily seen. In particular the controllers will be designed to be robust for a changing metacentric height (GM) which may change during a voyage due to consumption of fuel, changes to the ballast and change of mass and location of the cargo. The model used for this design exercise was previously described in Blanke and Jensen [1].

[1] Industrial Control Centre, Department of Electrical and Electronic Engineering, University of Strathclyde, Glasgow, United Kingdom. *e-mail*: gerald@icu.strath.ac.uk

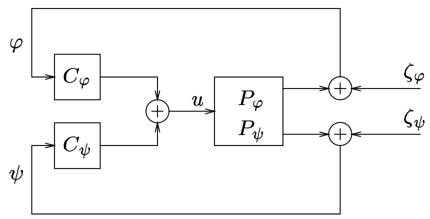

Fig. 1. Closed-loop for rudder roll damping.

2. CLOSED-LOOP OBJECTIVES

The feedback structure is shown in Fig. 1 with the roll controller (C_φ) and the yaw controller (C_ψ). The outputs of the controllers are summed to form the command signal to the rudder. The linear design system includes the output disturbances ζ_φ and ζ_ψ for the roll and yaw respectively. The closed-loop sensitivities which relates the disturbances to the roll and yaw are hence:

$$\begin{bmatrix} S_{\varphi\varphi} & S_{\varphi\psi} \\ S_{\psi\varphi} & S_{\psi\psi} \end{bmatrix} = \frac{1}{1+P_\varphi C_\varphi + P_\psi C_\psi} \begin{bmatrix} 1+P_\psi C_\psi & -P_\varphi C_\psi \\ -P_\psi C_\varphi & 1+P_\varphi C_\varphi \end{bmatrix} \quad (1)$$

Figure 2 shows the desired frequency objectives for the sensitivity magnitudes. The roll sensitivity $S_{\varphi\varphi}$ should have an upper bound of a bandstop filter between frequencies $\omega_{\varphi l}$ and $\omega_{\varphi u}$ with a minimum attenuation of α_φ dB. Outwith that frequency range the peak sensitivity should be less than $M_{\varphi\varphi}$. The yaw sensitivity $S_{\psi\psi}$ should have low frequency attenuation below $\omega_{\psi b}$ ($\omega_\psi < \omega_{\varphi l} < \omega_{\varphi u}$) and above that frequency the peak sensitivity should be less than $M_{\psi\psi}$. The off diagonal sensitivities are specified by a constant upper bound.

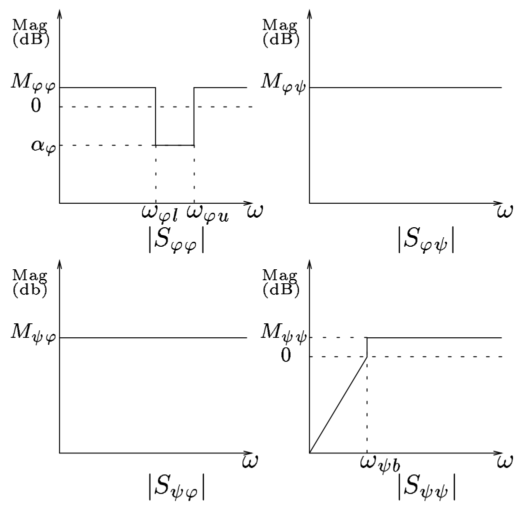

Fig. 2. Sensitivity frequency objectives.

3. DESIGN CONSTRAINTS

It is possible to quantify the fundamental limitations on the achievable closed-loop performance. As well as giving guidelines for the control design these performance limitations may also indicate when the performance specifications are unachievable and the open-loop plant should be modified (redesign the ship). For the rudder roll damping problem the limitations are due to an unstable pole and zero (analytic constraint) and the fact that yaw and roll designs need to have frequency separation (algebraic constraint) since the rudder is the only actuator. The algebraic constraint is fairly transparent since it involve design tradeoff at the same frequencies. A more subtle limitation is the analytical limitation due to unstable poles and zeros which involves design tradeoff at different frequencies.

For a function G there will exist an all-pass function G_{ap} and a minimum-phase function G_{mp} such that $G = G_{ap}G_{mp}$ where G_{ap} is the product of all factors of the form $\frac{s-s_0}{s+\bar{s}_0}$, $\mathrm{Re}\, s_0 > 0$. The separation of a sensitivity function into an all-pass and a minimum-phase part can be used with the **Poisson Integral Formula** [2]:

$$\log|S_{mp}(s_0)| = \frac{1}{\pi}\int_{-\infty}^{\infty} \log|S(j\omega)| \frac{\sigma_0}{\sigma_0^2 + (\omega-\omega_0)^2} d\omega \quad (2)$$

This relationship can be used to find a lower bound on the maximum sensitivity which is due to a decrease in the sensitivity over a different frequency range (the *waterbed* effect). Figure 3 shows the sensitivity being reduced at least over the range ω_1 to ω_2 with a maximum sensitivity of M_1 over this frequency range and a maximum magnitude over all frequencies of M_2. $M_1 = \max|S(j\omega)|$, $\omega_1 \le \omega \le \omega_2$, $M_2 = \|S\|_\infty$. If P has a zero at z with $\mathrm{Re}\, z > 0$ then $S(z) = 1$, $S_{mp}(z) = S_{ap}(z)^{-1}$ and $\log|S_{ap}(z)^{-1}| = 0$. A less conservative bound on the peak sensitivity may be found by assuming that the peak occurs close to the sensitivity reduction or that the sensitivity is unity at low ($\omega < \omega_l$) and high frequencies ($\omega > \omega_h$) as in Fig. 3 which gives the following inequality when the integral of $\log|S(j\omega)|$ is approximated by using the idealised bandstop filter:

$$\frac{\pi}{2}\log|S_{ap}(z)^{-1}| \le \left[\tan^{-1}\left(\frac{\omega_2}{\sigma_0}\right) - \tan^{-1}\left(\frac{\omega_1}{\sigma_0}\right)\right]\log(M_1) + \left[\tan^{-1}\left(\frac{\omega_1}{\sigma_0}\right) - \tan^{-1}\left(\frac{\omega_l}{\sigma_0}\right) + \tan^{-1}\left(\frac{\omega_h}{\sigma_0}\right) - \tan^{-1}\left(\frac{\omega_2}{\sigma_0}\right)\right]\log(M_2)$$

$$\log|S_{ap}(z)^{-1}| \le c_1\log(M_1) + c_2\log(M_2) \quad (3)$$

with $c_2 = 1 - c_1$, therefore the maximum sensitivity has a lower bound of:

$$\|S\|_\infty = M_2 \ge M_p = S_{ap}(z)^{\frac{-1}{1-c_1}} M_1^{\frac{-c_1}{1-c_1}} \ge 1 \quad (4)$$

Assuming ω_1 and ω_2 are constant the worst case peak sensitivity with respect to the location of the RHP-zero will occur when c_1 is a maximum which is at $\sigma_0 = \sqrt{\omega_1\omega_2}$. Instead of using the Poisson integral together with piecewise approximations of the sensitivity to find a lower bound for the peak it could be used to analysis an idealised case. If the trough of the sensitivity is an ideal bandstop then the location and width of the peaks can be selected and the peak sensitivity calculated. Figure 4 shows an ideal piecewise sensitivity which has a bandwidth and attenuation close to the actual sensitivity using the controller designed in section 5. The peaks of the calculated ideal sensitivity and the actual sensitivity are fairly close. One reason for this good match is that the actual sensitivity is nearly symmetrical in shape with two peaks of roughly the same magnitude. This enables a quantitative assessment to be made of the cost of rudder-roll reduction in terms of the roll amplification at other frequencies without actually going through the design process.

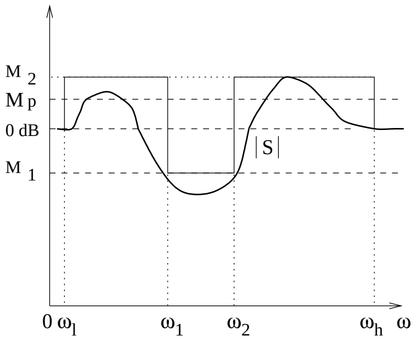

Fig. 3. Sensitivity for unstable zero with bound.

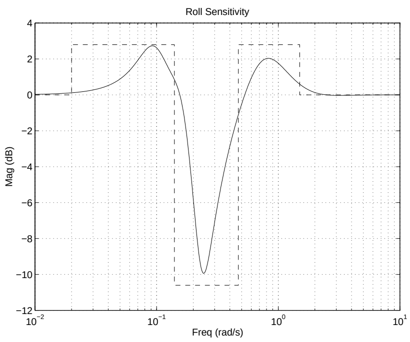

Fig. 4. Sensitivity approximation.

4. QUANTITATIVE FEEDBACK THEORY

Quantitative Feedback Theory (QFT) is a powerful robust control design technique developed by Isaac Horowitz [5]. The philosophy of Horowitz was that the principle reason for the use of feedback is plant uncertainty due to parameters and disturbance. QFT can be described as a transparent technique which uses the uncertainty upfront and reveals the tradeoff between performance specifications, plant uncertainty and the complexity of the controller. The basic objective of QFT is to design a SISO controller (cascaded for MIMO problems) which will have robust stability and robust performance for parametric uncertainty and will have the minimum bandwidth and complexity.

In QFT it is assumed that the plant uncertainty is represented by a set of templates $\mathcal{P}$ on the complex plain (polar form) within each is enclosed all possible frequency responses $P(j\omega_k)$ for some frequency ω_k. For each frequency the set $\mathcal{P}_\omega$ should consist of a finite number of elements therefore $\mathcal{P}_\omega$ should be obtained by using a discrete grid of uncertain parameters. The performance specifications consists of constraints ($W(\omega)$) on the magnitude of a closed-loop frequency response $F(s)$.

If the controller is $C(s)$ then the main process in QFT is translating the frequency domain specification W on the uncertain feedback system into bounds in the complex plain (or Nichols chart) where the nominal loop transmission ($L_0 = P_0 C : P_0 \in \mathcal{P}_\omega$) should lie within.

A bound is obtained by determing all possible positions on the Nichols chart which the uncertainty template of $\mathcal{P}(j\omega)$ can be translated without rotation such that the performance specification $F(s)$ satisfies its magnitude bound of $W(\omega)$. In the past this was a manual graphical task in the Nichols chart which made the calculation of bounds very laborious. With the advent of computer packages the bounds could be found by numerical searches and the state of the art method is now via quadratic inequalities implemented in [3]. To demonstrate this the bound calculation is shown for an output disturbance rejection problem. If the plant and controller in polar form is $P = pe^{j\theta}$ and $C = ce^{j\phi}$ respectively then the performance constraint is:

$$\left|\frac{1}{1 + cpe^{j(\phi+\theta)}}\right| \leq W(\omega) \tag{5}$$

Square both sides and evaluate the magnitude gives:

$$\left|\frac{1}{c^2p^2 + 2cp\ \cos(\phi+\theta) + 1}\right| \leq W(\omega)^2 \tag{6}$$

Rearranging gives the quadratic inequality which maps the uncertain plant and the closed-loop specification into the QFT bounds:

$$c^2[p^2]{+}2c[p\ cos(\phi+\theta)]{+}[1{-}W(\omega)^{-2}] \geq 0 \tag{7}$$

For a plant $P \in \mathcal{P}$, a frequency ω and the controller phase ϕ the unknown parameter in the inequality is $c = |C(\jmath\omega)|$. If the quadratic inequality is considered an equality then it has two solutions $\overline{c}(\phi)$ and $\underline{c}(\phi)$ which gives the range of the controller c magnitude for a specific controller phase ϕ. If the uncertain plant is defined by the set $\mathcal{P} = \{P_1(s), \dots, P_n(s)\}$ and the controller phase is the discrete set $\Omega = \{\phi_1, \dots, \phi_k\}$ then the bound for the frequency ω over the phase range $\phi \in \Omega$ with $P_0(s) \in \mathcal{P}$ and $\gamma_0 = \phi + \theta_0$ is:

$$\overline{L}_\omega(\gamma_0) = p_0 c_{\max}(\phi) \tag{8}$$

$$\underline{L}_\omega(\gamma_0) = p_0 c_{\min}(\phi) \tag{9}$$

$$c_{\max}(\phi) = \max[\overline{c}(P_i)], \quad i = 1, \dots, n. \tag{10}$$

$$c_{\min}(\phi) = \min[\underline{c}(P_i)], \quad i = 1, \dots, n. \tag{11}$$

Although the bounds can be calculated in terms of the controller gain and phase it is necessary to do the loopshaping using the loop gain L so robust stability bounds can be used. The L bounds are obtained by multiplying the controller bounds by the nominal P_0 which is any one of the plants from the set $\mathcal{P}$. In practice there will be a number of performance specifications: robust performance, robust stability, control effort each of which will produce a bound for each of the frequencies chosen. For each frequency the final bound will be the boundary of the union of the set of bounds.

Design Specification:
The design specifications can be in the time domain and translated into the frequency domain although some conservativeness may be introduced. Or the specifications may be directly in the frequency domain as constraints on the disturbance sensitivity, control sensitivity and robustness margins.

Representation of Uncertainty:
For a discrete number of chosen frequencies the gain and phase are needed for a discrete number of different plants. This information could be obtained from changing parameters in a linear model or directly from frequency response data from the physical plant. The uncertainty templates on the Nichols chart should be a smooth approximation. For most problems it is sufficient to use only the boundary of the templates and not internal points.

Nominal Plant Selection:
Any of the plants can be chosen as the nominal one although it may be convenient to use the plant which has the most probable dynamics.

Bound Generation:
Once bounds have been computed it may be apparent that the selection of the frequency array for the templates may not be ideal. Frequencies should only be used where templates change shape significantly which is usually not at high or low frequencies. If after the design is completed successfully in terms of the bounds on the Nichols diagram but on a Bode diagram the closed-loop does not meet the specifications at some frequencies, then these frequencies should be added for bound recalculation.

Loop Generation:
The open-loop frequency response $L(j\omega) = P_0(j\omega)C(j\omega)$ is shaped by adding dynamic elements to the nominal plant such that open-loop function lies on or above the bounds. If the bounds are satisfied for the nominal plant then the specifications are satisfied for all plants described by the uncertainty.

5. RUDDER ROLL DESIGN

The closed-loop specifications are defined by: $\omega_{\varphi l}$=0.2rad/s, $\omega_{\varphi u}$=0.4rad/s, $M_{\varphi\varphi}$= -2db, α_φ=5db, $M_{\varphi\psi}$= 20db, $\omega > 0.05 = \omega_{\psi b}$ rad/s, $S_{\psi\psi} < M_{\psi\psi}$ = 10db, $\omega < 0.05$rad/s, $S_{\psi\psi} < 20log_{10}(400(\omega^2 + 0.001^2))$ db, $M_{\psi\varphi}$= 0db. The uncertainty sets for yaw ($\mathcal{P}_\psi$) and roll ($\mathcal{P}_\varphi$) are constructed from the frequency responses for GM $= \{0.55, 0.6, 0.7, 0.83, 0.9, 1.0, 1.1, 1.2\}$ [m] (Fig. 5) at 13 frequencies.

5.1 *Yaw Control*

The objective is to find a controller which rolls off well before the roll natural frequency, of low

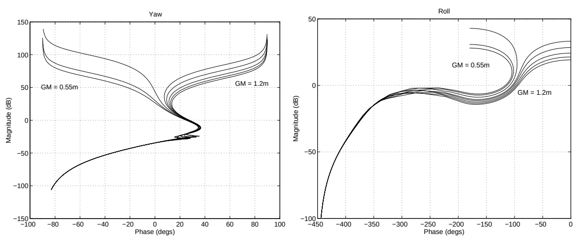

Fig. 5. Variation of P_ψ and P_φ with GM.

complexity such that the following specification is satisfied:

$$\left|\frac{1}{1 + P_\psi(j\omega)C_\psi(j\omega)}\right| \leq S_{\psi\psi}(\omega), \quad \forall P_\psi \in \mathcal{P}_\psi \tag{12}$$

A controller (Fig. 7) which achieves this specification is:

$$C_\psi = \frac{-12(s + 0.4)}{(s + 1)(s + 1)} \tag{13}$$

Figure 6 shows the nominal loop (L_0^ψ) satisfying the bounds. The negative controller sign is to shift the nominal loop into the right phase region, The zero ($z = -0.4$) provide phase-lead to satisfy the high frequency bounds which are the stability bounds. The two poles ($p = -1$) are there to roll off the controller gain before the frequency region where the roll controller is significant. The controller is simple and the robust performance bounds are satisfied by using the gain of 12. The specification here is not the true yaw sensitivity when the roll loop is closed but the best approximation since the roll controller is not yet designed. Part of the roll design specifications will be to make sure that the true sensitivity meets the same specifications. If it doesn't then the yaw controller would have to be designed again to prevent the roll controller design being compromised.

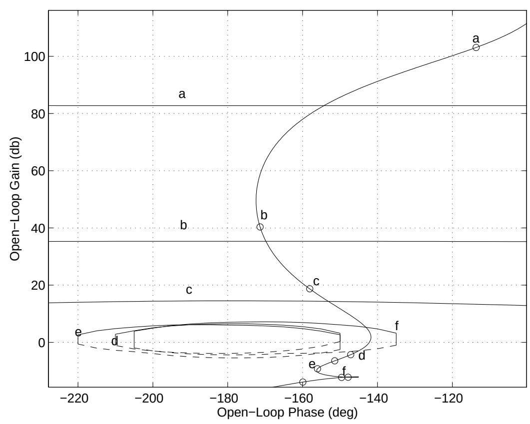

Fig. 6. Nominal loop for yaw, L_0^ψ with bounds.

5.2 *Roll Controller Design*

The objectives are to find a controller of minimum complexity such that the following specifications are satisfied:
Bound on the gain and phase margins for the both the yaw and roll loops being closed:

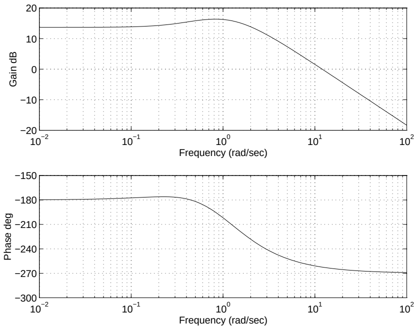

Fig. 7. Frequency response of yaw controller, C_ψ.

$$\left|\frac{1}{1+P_\psi(j\omega)C_\psi(j\omega)+P_\varphi(j\omega)C_\varphi(j\omega)}\right| \le 2,\ \forall P_\psi \in \mathcal{P}_\psi,\ \forall P_\varphi \in \mathcal{P}_\varphi$$

Roll damping sensitivity:

$$\left|\frac{1+P_\psi(j\omega)C_\psi(j\omega)}{1+P_\psi(j\omega)C_\psi(j\omega)+P_\varphi(j\omega)C_\varphi(j\omega)}\right| \le S_{\varphi\varphi}(\omega),\ \forall P_\psi \in \mathcal{P}_\psi,\ \forall P_\varphi \in \mathcal{P}_\varphi$$

Preservation of yaw sensitivity:

$$\left|\frac{1+P_\varphi(j\omega)C_\varphi(j\omega)}{1+P_\psi(j\omega)C_\psi(j\omega)+P_\varphi(j\omega)C_\varphi(j\omega)}\right| \le S_{\psi\psi}(\omega),\ \forall P_\psi \in \mathcal{P}_\psi,\ \forall P_\varphi \in \mathcal{P}_\varphi$$

Roll-yaw crossover sensitivity:

$$\left|\frac{-P_\varphi(j\omega)C_\psi(j\omega)}{1+P_\psi(j\omega)C_\psi(j\omega)+P_\varphi(j\omega)C_\varphi(j\omega)}\right| \le S_{\varphi\psi}(\omega),\ \forall P_\psi \in \mathcal{P}_\psi,\ \forall P_\varphi \in \mathcal{P}_\varphi$$

Yaw-roll crossover sensitivity:

$$\left|\frac{-P_\psi(j\omega)C_\varphi(j\omega)}{1+P_\psi(j\omega)C_\psi(j\omega)+P_\varphi(j\omega)C_\varphi(j\omega)}\right| \le S_{\psi\varphi}(\omega),\ \forall P_\psi \in \mathcal{P}_\psi,\ \forall P_\varphi \in \mathcal{P}_\varphi$$

A controller (Fig.9) which achieves these specifications is:

$$C_\varphi = \frac{-800(s+0.1)^2(s^2+0.0945s+0.021)}{(s+1)^2(s^2+8s+16)(s^2+0.145s+0.021)} \qquad (14)$$

Figure 8 shows the nominal loop (L_0^φ) and the bounds. The Nichols plot is single-sheeted since it only has a phase range of 360°. Since the nominal loop has a phase range greater than 360° it wraps around the plot such that frequency ω_e is after ω_d. The bounds show the resonant characteristics of the system needed for performance while the bounds around the -1 point show the robust margins. Frequency point (a) should lie outwith the contour of bound (a). This is a consequence of the robust margin not being strictly satisfied and does not affect the robust performance. Its possible that a more complex controller could satisfy this bound or the specifications could be changed but the violation is not serious to the design. The significant controller elements are $C_\varphi = \frac{-800(s+0.1)(s+0.1)}{(s+1)(s+1)}$. The elements $\frac{(s^2+0.0945s+0.021)}{(s^2+0.145s+0.021)}$ are used to achieve robust performance at (b) and the denominator element $(s^2+8s+16)$ is used to roll the controller off at high frequencies.

The design of the controller follows a similar strategy as suggested by Horowitz for non-minimum phase feedback systems [4]. The strategy is to have multiple gain cross-over frequencies and to swing $L(j\omega)$ clockwise to a region where $|L(j\omega)| > 1$ such that -1 is not encircled. The principle elements of the controller are used at the low frequency region to shift the phase such that $-180°$ is passed before the gain is greater than unity. The next part of the controller is phase lead to postpone the next passing of $-180°$ until the gain is less than unity at the second cross-over frequency. The complex poles and zeros in the full controller are there such that this principle holds for the range of GM to achieve robust performance.

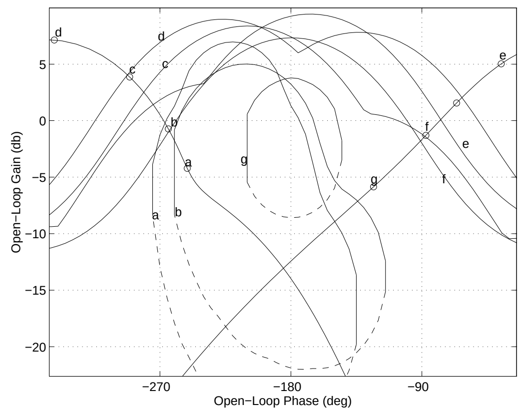

Fig. 8. Nominal loop for roll, L_0^φ with bounds.

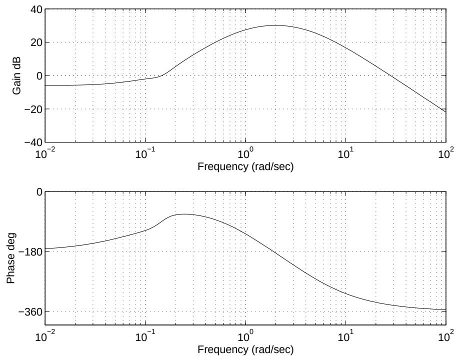

Fig. 9. Frequency response of roll controller, C_φ.

5.3 *Robust Performance Verification*

The closed-loop sensitivities are compared with the specifications in Figures 10 and 11. All the frequency domain objectives have been met. The roll sensitivity attenuation extends far below the bound which is not quite true to the principles of QFT in that the controller should have the minimum gain and be as close as possible to the bound. The actually roll damping specified was not very demanding but it was realised that since a low order controller was to be used that the roll attenuation would be a lot greater since the bandstop filter would be close to a notch and not an ideal trough. The specification could have been chosen to be closer to the expected shape of the sensitivity but it would not have affected the design.

5.4 *Simulation Results*

The controller is evaluated using a nonlinear simulation with GM = 0.55m, GM = 0.83m and GM

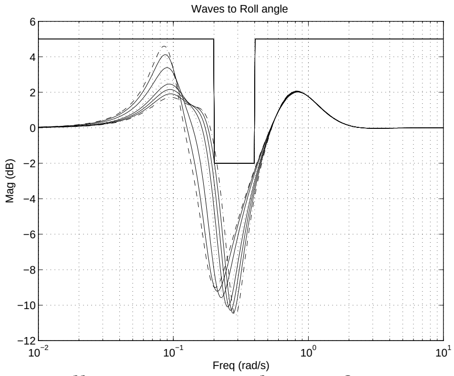

Fig. 10. Roll sensitivity with specification.

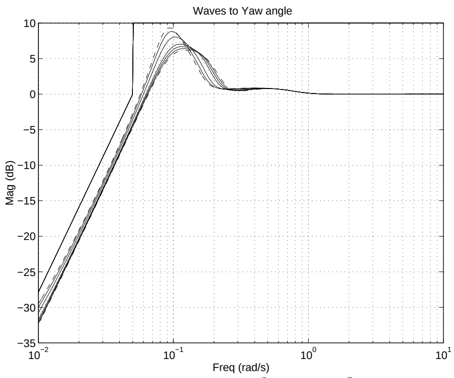

Fig. 11. Yaw sensitivity with specification.

= 1.2m. The waves have a significant height of $h_{1/3}$ = 3m, a period T_w = 8s and an angle of $\chi = 20°$. The ship is at its nominal speed of $U = 12.7m/s$ and the rudder has constraints of $|\delta|_{max} = 35$ and $|\dot{\delta}|_{max} = 4.6°/s$. Figure 12 shows the results for GM = 0.55m with and without the roll controller used (- - only yaw controller). For this GM in this sea state the rudder is saturating due to the roll controller. The roll reduction ratio (rr_ϕ=1- $\frac{\text{roll control on}}{\text{roll control off}}$) is $rr_\phi = 0.2$ during rudder saturation and $rr_\phi = 0.4$ at other times. For GM = 0.83m (Fig.13) $rr_\phi = 0.52$ and for GM = 1.2m (Fig.14) $rr_\phi = 0.53$. The limited results do demonstrate that the roll controller has the desired robust performance for variations in GM while controlling the ships heading adequately.

6. CONCLUSIONS

The demanding problem of designing controllers to use the rudder for simultaneous course keeping and roll reduction was made more transparent by using approaches which give more insight to the design process and tradeoffs. A formula for complex functions was used to quantify the limitations of performance for roll damping before a controller was designed and QFT was used to design low order robust controllers. Future work should incorporate the rudder constraints into the QFT design process and increase the number of uncertain parameters.

7. REFERENCES

[1] M. Blanke and A. G. Jensen, *Dynamic Properties of Container Vessel with Low Metacentric Height*, Trans Inst Measurement & Control, Vol 19, No. 2, pp.78-93, 1997.

[2] J. C. Doyle, B. A. Francis and A. R. Tannenbaum, *Feedback Control Theory*, Macmillan, 1992.

[3] C. Borghesani, Y. Chait and O. Yaniv, "Quantitative Feedback Theory Toolbox", *The Math Works Inc*, 1994.

[4] I. Horowitz, "Design of Feedback Systems with Non-minimum-phase unstable plants", *Int. J. Systems Sci.*, Vol 10., No. 9, 1979.

[5] I. Horowitz, "Survey of Quantitative Feedback Theory (QFT)", *Int. J. Control*, Vol 53., No. 2, 1991.

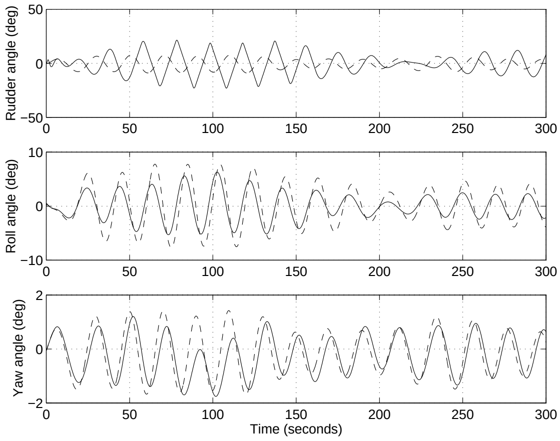

Fig. 12. Ship response for GM = 0.55m.

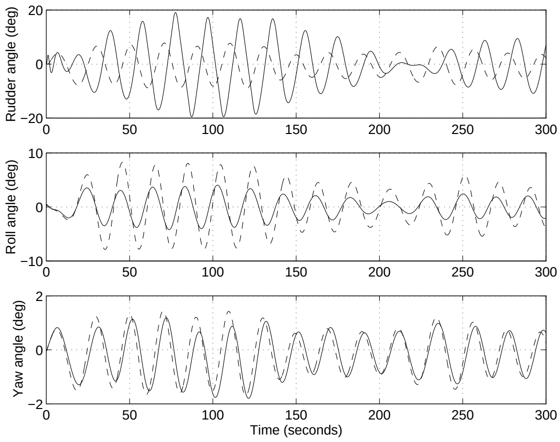

Fig. 13. Ship response for GM = 0.83m.

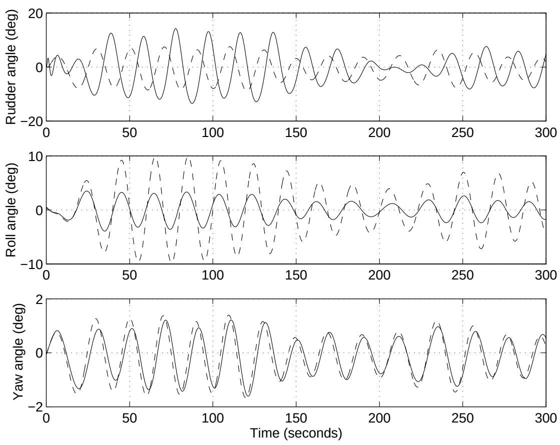

Fig. 14. Ship response for GM = 1.2m.